

Marquette University
e-Publications@Marquette

Chemistry Faculty Research and Publications

Chemistry, Department of

1-1-2008

Kinetic, Spectroscopic, and X-Ray Crystallographic Evidence for the Cooperative Mechanism of the Hydration of Nitriles Catalyzed by a Tetranuclear Ruthenium- μ -oxo- μ -hydroxo Complex

Chae S. Yi

Marquette University, chae.yi@marquette.edu

Tonya N. Zeczycki

University of Wisconsin - Madison

Sergey V. Lindeman

Marquette University, sergey.lindeman@marquette.edu

Accepted version. *Organometallics*, Vol. 27, No. 9 (2008): 2030-2035. DOI. © 2008 American Chemical Society. Used with permission.

Marquette University

e-Publications@Marquette

Chemistry Faculty Research and Publications/College of Arts and Sciences

This paper is NOT THE PUBLISHED VERSION; but the author's final, peer-reviewed manuscript. The published version may be accessed by following the link in the citation below.

Organometallics, Vol. 27, No. 9 (2008): 2030-2035. [DOI](#). This article is © American Chemical Society and permission has been granted for this version to appear in [e-Publications@Marquette](#). American Chemical Society does not grant permission for this article to be further copied/distributed or hosted elsewhere without the express permission from American Chemical Society.

Kinetic, Spectroscopic, and X-Ray Crystallographic Evidence for the Cooperative Mechanism of the Hydration of Nitriles Catalyzed by a Tetranuclear Ruthenium- μ -oxo- μ -hydroxo Complex

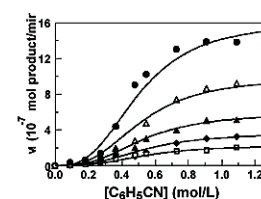
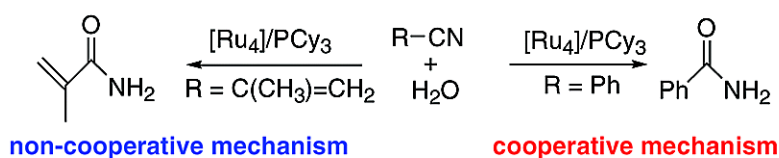
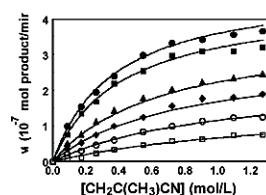
Sergey Lindeman

Department of Chemistry, Marquette University, Milwaukee WI

Chae Yi

Department of Chemistry, Marquette University, Milwaukee WI

Abstract



The tetranuclear ruthenium-oxo-hydroxo-hydride complex $\{[(PCy_3)(CO)RuH]_4(\mu_4-O)(\mu_3-OH)(\mu_2-OH)\}$ (**1**) was found to be a highly cooperative catalyst for the nitrile hydration reaction. The cooperative mechanism of the hydration of benzonitrile was established by Hill inhibition kinetics. The treatment of a nitrile substrate with complex **1** led to the catalytically relevant nitrile-coordinated tetraruthenium complex **3**. The X-ray structure of the nitrile-coordinated complex **3** showed a considerably “relaxed” tetrameric core structure compared to that of **1**. The hydration of *para*-substituted benzonitriles *p*-X-C₆H₄CN with an electron-withdrawing group (X = Cl, Br, CO₂H, CF₃) exhibited cooperative kinetics, as indicated by the sigmoidal saturation kinetics, while the hydration of nitriles with an electron-donating group (X = OH, OMe, *t*-Bu, CH₃) obeyed Michaelis–Menten saturation kinetics. The formation of a ruthenium hydride species was observed during the hydration of methacrylonitrile, and its monomeric nature was established by using DOSY NMR techniques.

Introduction

Designing highly cooperative metal catalysts that can mimic nature’s allosteric metalloenzymes has been a challenging goal for synthetic chemists.¹ While multinuclear transition metal complexes have long been regarded as promising model systems for promoting the cooperative activity for a number of synthetically useful catalytic transformations,² well-defined examples of synthetic metal catalysts that exhibit high cooperative activity remain quite rare. Moreover, detailed mechanistic understandings of the origin of cooperativity have not been established for many of these catalytic reactions. Recently, a number of both homo- and heterometallic catalytic systems have been shown to exhibit cooperative effects in mediating different types of catalytic reactions.³ A supramolecular approach has been proven to be a particularly effective tool in promoting allosteric effects for the asymmetric epoxide ring-opening and other related reactions.⁴ Heterobimetallic chiral rare earth metal catalysts have also been successfully utilized for cyanosilylation and an aldol-type condensation as well as for conjugate addition reactions.⁵ The synergistic cooperative effects of di- and trimetallic complexes have been demonstrated for both C–C bond activation⁶ and alkyne insertion reactions⁷ under stoichiometric reaction conditions.

One of the distinguishing features of allosteric enzymes is the sigmoidal saturation kinetics, which results from the cooperative interaction among multiple numbers of active sites.⁸ Despite considerable synthetic efforts to mimic the allosteric activity of natural enzymes, only a few multinuclear metal catalysts have been shown to obey sigmoidal saturation kinetics.^{1b,9} We recently discovered that the tetranuclear ruthenium complex $\{[(PCy_3)(CO)RuH]_4(\mu_4-O)(\mu_3-OH)(\mu_2-OH)\}$ (**1**) is a highly cooperative catalyst for the transfer dehydrogenation of alcohols, as indicated by sigmoidal saturation kinetics.¹⁰ Unfortunately, the detailed mechanistic study was hampered by a lack of detectable intermediate species and difficulty in elucidating the origin of cooperativity. To further discern the cooperative mechanism of **1**, we have begun to explore the activity of **1** for other catalytic reactions that give both reliable kinetics and detectable intermediate species. This report delineates detailed kinetic and spectroscopic analyses for the cooperative mechanism of **1** in mediating the nitrile hydration reaction.

Results and Discussion

Scope of the Nitrile Hydration Reaction

Due to strong coordinating ability of nitriles, we initially reasoned that the nitrile hydration reaction might be suitable for detecting reactive intermediate species. Indeed, an initial activity survey showed that complex **1** is a highly effective catalyst for the nitrile hydration reaction. Thus, the treatment of a

nitrile (1–3 mmol) with an excess amount of H₂O (10–20 equiv) in the presence of **1** (1–2 mol %) at 80–90 °C cleanly produced the amide product **2** (eq 1).¹¹ Two distinct color patterns of the solution were observed depending on the nature of the nitrile substrates: the color of the solution turned pale yellow for nitriles with aliphatic and electron-releasing groups, while it remained red-brown (due to the color of **1**) for the aryl-substituted nitriles (Table 1). For the hydration of acrylic nitriles, acrylic amides were selectively formed without giving any significant amounts of 1,4-addition or other byproducts. The chemoselective catalytic hydration of nitriles to amides is a highly desired transformation, due in part to the synthetic utility of acrylic amides in industrial processes.¹²

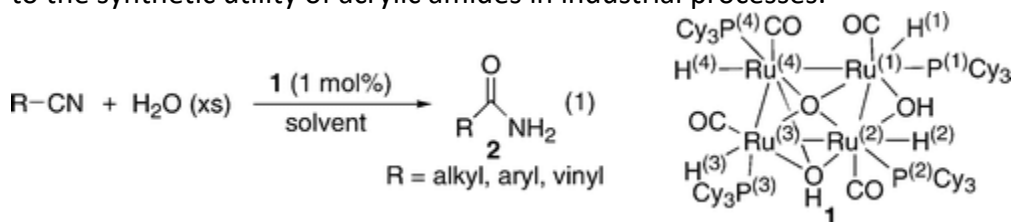
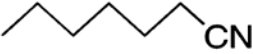
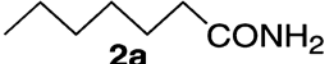
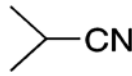
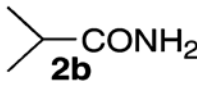
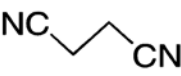
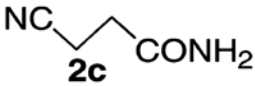
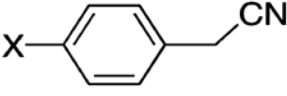
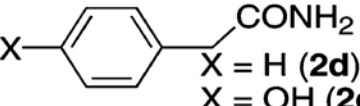
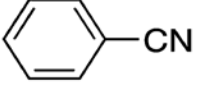
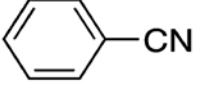
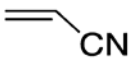
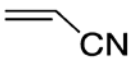
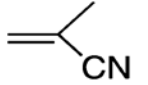
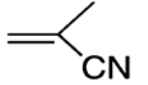
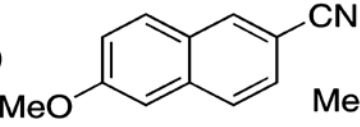
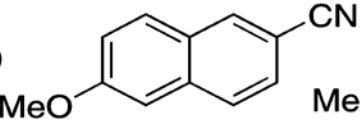
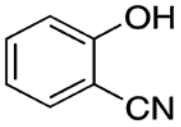
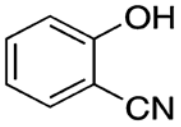
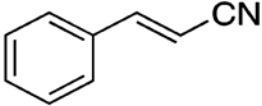
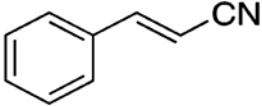
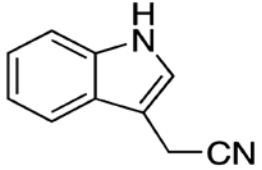
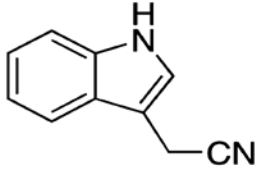
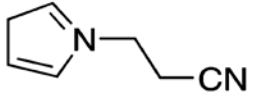
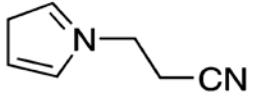
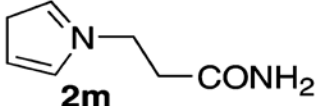


Table 1. Catalytic Hydration of Nitriles to Amides^a

entry	nitrile	product	solvent	t (h)	color	yield (%) ^b
1 ^c		 2a	i-PrOH	12	yellow	78
2		 2b	THF	12	yellow	84
3		 2c	i-PrOH	16	yellow	98
4		 X = H (2d)	i-PrOH	14	yellow	98
5		 X = OH (2e)	i-PrOH	6	yellow	92
6		 2f	i-PrOH	8	red	99
7		 2g	DME	6	red	98
8		 2h	i-PrOH	8	yellow	98
9		 2i	DME	14	red	89
10		 2j	i-PrOH	8	yellow	94
11 ^c		 2k	DME	6	red	97
12		 2l	DME	18	yellow	98
13		 2m	DME	6	yellow	98

^a Reaction conditions: nitrile (1–3 mmol), 10–20 equiv of H₂O, **1** (1 mol %), solvent (2–3 mL), 80–90 °C.

^b Isolated yield. ^c 1–2 equiv of H₂O was used.

Table 2. Kinetic Parameters Obtained for the Hydration of *p*-X-C₆H₄CN

X substituent	V_{\max} (10^{-6} mol product/min)	K_m (mM)
OH	1.18	327
OMe	1.59	128
Me	5.46	176
<i>t</i> -Bu	5.49	126
Cl	1590	48
Br	1320	42
CO ₂ H	3120	32
CF ₃	9580	30

Kinetic Study

Since the cooperative activity of the catalyst **1** was previously observed for the red-brown-colored solutions,¹⁰ the kinetics of the benzonitrile hydration reaction (red-brown-colored solution) was compared to that of methacrylonitrile (yellow-colored solution). The rate of the product formation was measured by monitoring the appearance of the amide product by NMR. The initial rate of the hydration reaction for each concentration was determined from the first-order plots of the product formation vs time.

The initial rate (v_i) vs [PhCN] plots for the hydration of benzonitrile exhibited a sigmoidal nature of the saturation kinetics. Both $K_{0.5} = 148$ mM and the Hill coefficient of $n = 3.2 \pm 0.2$ were obtained from fitting the data to the Hill equation, $v_i/V_{\max} = [\text{PhCN}]^3/(K_{0.5}^3 + [\text{PhCN}]^3)$. A relatively high Hill coefficient of 3 suggested the presence of three available and interacting substrate binding sites.¹³ In contrast, the plot of the initial rate vs [methacrylonitrile] gave a hyperbolic saturation curve. The fitting of the data to the Michaelis–Menten equation gave $K_m = 533$ mM, which was more than 3 times larger than the $K_{0.5}$ of benzonitrile. A relatively high value of K_m for methacrylonitrile means that the binding affinity of methacrylonitrile is lower than that of benzonitrile.

The phosphine inhibition kinetics was performed to further establish the cooperative activity of the catalyst **1**. The kinetic plots of initial rate (v_i) as a function of [PhCN] at different [PCy₃] showed that the cooperative activity was effectively lost upon the addition of 1.5 equiv of PCy₃ (Figure 1A). Using the Hill coefficient ($n = 3$) as a guideline, the cooperative Hill kinetic equation with three substrate-binding sites was successfully derived with the King–Altman method¹⁴ under rapid equilibrium conditions (Figure 1C).¹⁵ The inhibition data were globally fit to this equation using nonlinear regression techniques (ProStat V 4.1). The kinetic parameters, $K_m = 36 \pm 2$ mM and $K_i = 236 \pm 4$ mM, as well as the cooperativity factors, $\alpha = 0.5 \pm 0.1$ and $\beta = 1.9 \pm 0.4$, were obtained from this analysis. The positive α and β values are further evidence for the cooperative binding of the benzonitrile substrate; both of these values would be zero if there were no cooperative interactions among the substrate binding sites. In contrast, the analogous inhibition kinetic plots for the hydration of methacrylonitrile obeyed Michaelis–Menten saturation kinetics (Figure 1B). In this case, an excellent global fit of the experimental data to the two-site partially mixed Michaelis–Menten inhibition kinetic scheme was achieved, and $K_m = 553 \pm 3$ mM and $K_i = 132 \pm 4$ mM were obtained from the data analysis (Figure 1D).^{15, 16}

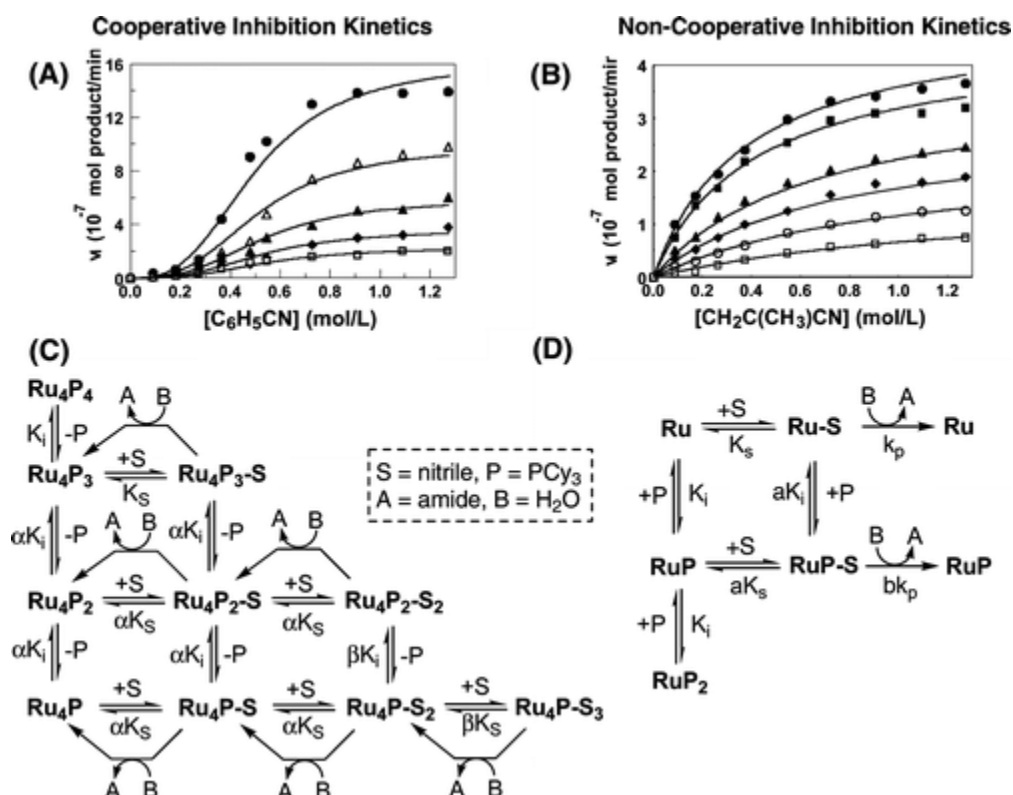


Figure 1. Cooperative vs noncooperative phosphine inhibition kinetic plots for the hydration of PhCN (A) and $\text{CH}_2=\text{C}(\text{CH}_3)\text{CN}$ (B): without added PCy_3 (\bullet), 0.16 equiv (\blacksquare), 0.25 equiv (Δ), 0.50 equiv of PCy_3 (\blacktriangle), 1.0 equiv of PCy_3 (\blacklozenge), 1.34 equiv (\circ), and 1.5 equiv of PCy_3 (\square). The Hill kinetic scheme with three substrate-binding sites (C) and the two-site Michaelis–Menten kinetic scheme (D).

Electronic Effects on the Cooperative vs Noncooperative Kinetics

To systematically probe the electronic effects on the cooperative activity, we next compared the kinetics of a series of *para*-substituted benzonitriles $p\text{-X-C}_6\text{H}_4\text{CN}$. As before, the initial rates were determined from pseudo-first-order plots of the rate of the product formation vs time for each nitrile substrates. The plot of the initial rate (v_i) vs $[\text{ArCN}]$ for the hydration of benzonitriles with an electron-withdrawing group ($\text{X} = \text{Cl}, \text{Br}, \text{CO}_2\text{H}, \text{CF}_3$) showed a sigmoidal saturation kinetics (Figure 2). The saturation kinetics was successfully fitted to the Hill equation ($v_i/V_{\text{max}} = [\text{ArCN}]^n / (K_{0.5}^n + [\text{ArCN}]^n)$ with the Hill coefficient of $n = 3$), and the color of the solution remained brown-red for all of these cases. In contrast, the analogous plots for the benzonitriles with an electron-donating group ($\text{X} = \text{OH}, \text{OMe}, \text{C}(\text{CH}_3)_3, \text{Me}$) gave hyperbolic saturation curves, and the color of the solution turned yellow after 20 min of heating at 80°C . The Michaelis–Menten kinetics ($v_i = [\text{ArCN}] / (K_m + [\text{ArCN}])$) was successfully used to fit the data for these cases (Figure 3).

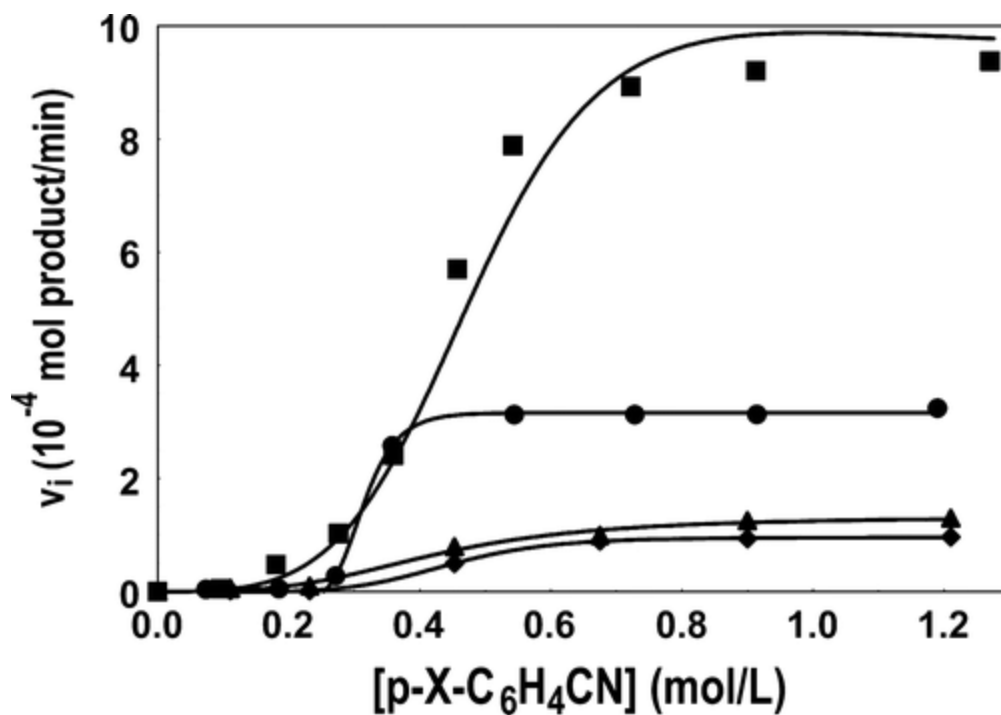


Figure 2. Plots of initial rate vs $[p\text{-X-C}_6\text{H}_4\text{CN}]$ that give cooperative kinetics: X = CF₃ (■), CO₂H (●) Br (▲), Cl (◆).

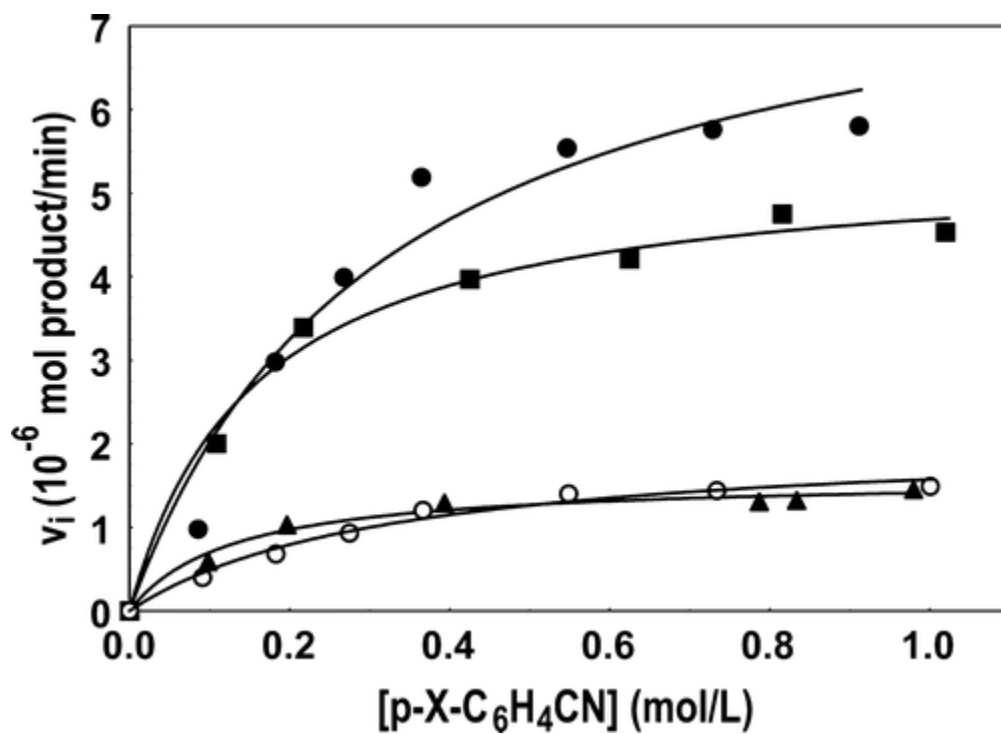


Figure 3. Plots of initial rate vs $[p\text{-X-C}_6\text{H}_4\text{CN}]$ that give noncooperative kinetics: X = *t*-Bu (●), CH₃ (■), OCH₃ (▲), OH (○).

The kinetic parameters, K_m and V_{max} , were obtained from the nonlinear regression analysis of the hydration kinetic data of *para*-substituted benzonitriles p -X-C₆H₄CN (Table 2). In general, the V_{max} of the nitriles with an electron-withdrawing group are 2–3 orders of magnitude higher than those with an electron-donating group. The corresponding K_m values are considerably smaller than the nitriles with an electron-donating group, indicating that the catalyst has a relatively high affinity for these substrates. These results showed that the electronic nature of the nitrile substrate plays a key role in dictating the cooperative vs noncooperative mechanism. We believe that the nucleophilic nature of the nitriles (and the corresponding amide products) is the major factor in influencing the stability of the tetrameric ruthenium core; that is, electron-rich and nucleophilic nitriles tend to promote the noncooperative mechanism by breaking up the tetrameric ruthenium core structure of the catalyst **1**.

Catalytically Relevant Nitrile-Coordinated Tetraruthenium Complex

We next examined the reaction of **1** with a nitrile substrate to gain new insights on the cooperative mechanism. Thus, the treatment of complex **1** (30 mg, 20 μ mol) with excess PhCN (8 μ L, 4 equiv) in C₆D₆ produced an equilibrium mixture of **1** and two new nitrile-coordinated complexes, **3a** and **3b**, in a 1:8:0.5 ratio, as monitored by NMR at room temperature (Figure 4, top spectrum).¹¹ Site-selective nitrile coordination to Ru(1) was established for both complexes from the analogous treatment of **1** with PhC¹⁵N (98% ¹⁵N), in which case, the H(1) hydride peaks of both **3a** and **3b** turned into apparent triplets (t, $J_{NH} = 15.3$ Hz) (Figure 2, bottom spectrum). The H(4) hydride peak of **3a** at $\delta -14.06$ (t, $J_{PH} = 19.1$ Hz) was found to couple to both P(3) and P(4), while the H(2) hydride peak of **3b** at $\delta -19.28$ (ddd, $J_{PH} = 28.6, 18.3, 3.4$ Hz) was coupled to both P(1) and P(4) in addition to P(2), as established by both ¹H–³¹P HSQC and ¹H–¹H COSY NMR analysis.

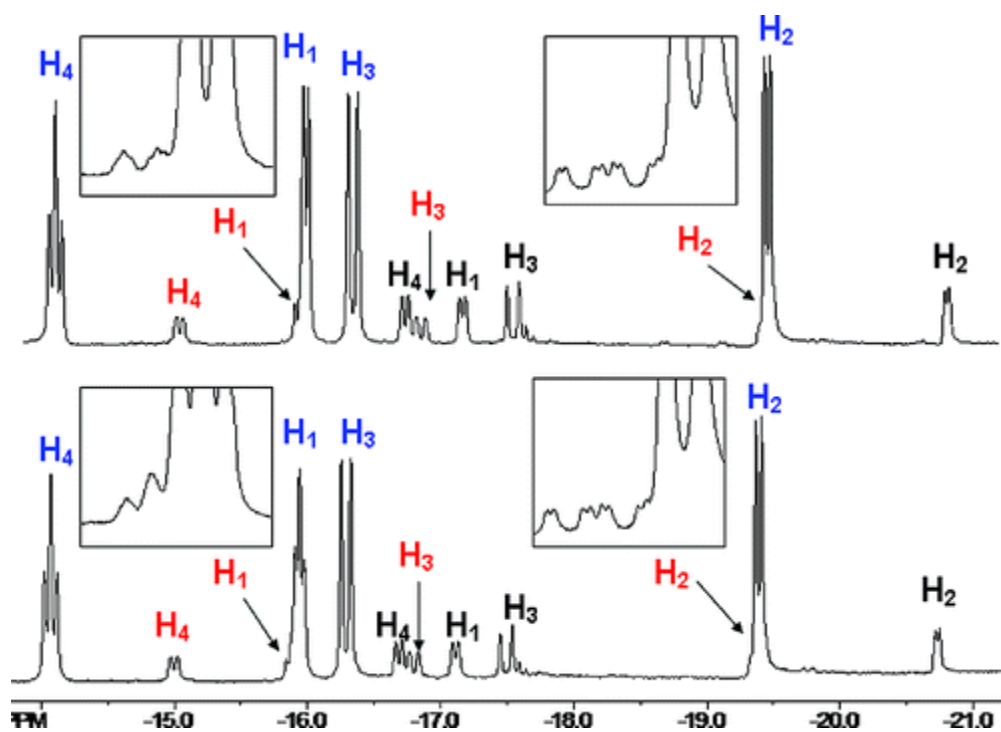


Figure 4. Metal hydride region of the ¹H NMR (400 MHz, toluene-*d*₈) spectra of the reaction of **1** with PhCN (top) and with PhC¹⁵N (bottom) at 20 °C. Color code: **1** (black), **3a** (blue), **3b** (red). Insets: expanded regions for H(1) and H(2) recorded in CD₂Cl₂.

The site-selective nitrile coordination to Ru(1) was further established by X-ray crystallography. Thus, the treatment of **1** with CH₃CN/CH₂Cl₂ at 0 °C led to the formation of single crystals of the nitrile-coordinated complex **3c** suitable for X-ray diffraction. The molecular structure of **3c** clearly showed the selective coordination of a single CH₃CN molecule to Ru(1) (Figure 5). Other notable structural features for the tetrameric core structure of **3c** compared to that of the parent complex **1** include (1) the conversion of the bridging μ_3 -OH into a μ_2 -OH, (2) the rearrangement of the terminal hydrides into bridging ones, and (3) a significant increase in the Ru(2)–Ru(3) and Ru(3)–Ru(4) bond distances, from 2.70–2.71 to 2.81–2.87 Å. The corresponding NMR spectroscopic patterns of the Ru–H and phosphorus signals of **3c** were virtually identical to those of **3a** and **3b**, indicating that the initial coordination of a single nitrile molecule to **1** is amenable to the observed structural changes in the solid state.¹⁷ We believe that the “relaxed” ruthenium core geometry of **3c** may be responsible for promoting the cooperative substrate binding to the neighboring Ru centers and increased catalyst activity. In support of this argument, the catalytic activity of isolated **3a/3b** was found to be nearly 4 times higher than **1** for the hydration of benzonitrile under similar conditions.

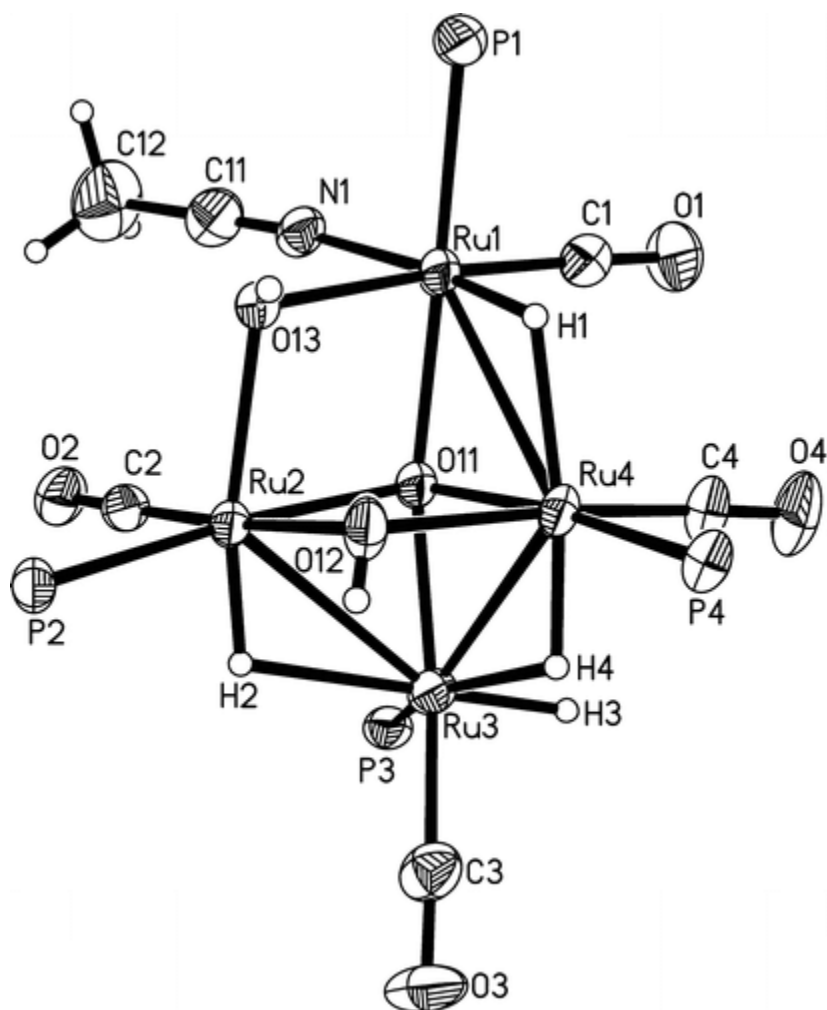


Figure 5. Molecular structure of **3c** drawn with 50% thermal ellipsoids. Cyclohexyl groups are omitted for clarity.

Mechanistic Considerations

The combined kinetic and spectroscopic analyses revealed new insights into the cooperative mechanism of **1** for the nitrile hydration reaction. The sigmoidal rate for the benzonitrile hydration

reaction has been successfully described by Hill inhibition kinetics with three substrate-binding sites. Both NMR and X-ray crystallographic data provided direct evidence for the initial site-selective nitrile coordination and its cooperative effect on the neighboring substrate-binding sites. The molecular structure of **3c**, which showed a more “relaxed” conformation of the core structure as indicated by the elongated bond length and the loss of μ -OH interaction compared to **1**, was induced by the site-selective coordination of a single nitrile molecule. A tantalizing mechanistic implication is that the “tight–relaxed” conformational change of the ruthenium core might be responsible for promoting the cooperative substrate binding and the increased catalytic activity. Such “allosteric” activity of **1** is both kinetically and functionally similar to those observed for natural allosteric proteins and enzymes, but has rarely been observed in synthetic systems.¹⁸

The nucleophilicity of the nitrile substrate was found to be the major factor for determining a cooperative vs a noncooperative mechanism. The kinetics of the hydration of a series of *para*-substituted benzonitriles *p*-X-C₆H₄CN indicated that the nitriles with an electron-withdrawing group consistently gave cooperative profiles as indicated by sigmoidal saturation kinetics, while the nitriles with an electron-rich group promoted a noncooperative mechanism, as indicated by the Michaelis–Menten saturation kinetics. One possible explanation for the different kinetic behavior is that electron-rich and nucleophilic nitriles (and the corresponding amide products) promote the breakup of the tetrameric ruthenium core into monomeric species and mediate noncooperative hydration reactions. These results are also consistent with the observation that the color of the solution remained red-brown for the hydration of electron-poor nitriles (due to the tetrameric color of **1**), whereas the color turned yellow for the hydration of electron-rich nitrile cases (due to the formation of monomeric species).

To obtain more definitive evidence for the nature of monomeric species, the structural elucidation of the “yellow Ru complex” was pursued. Thus, the treatment of **1** (30 mg, 20 μ mol) with an excess amount of CH₂=C(CH₃)CN (5 equiv) and H₂O (10 equiv) in acetone-*d*₆ was monitored by NMR. The color of the solution turned yellow within 10 min, and the hydride signals due to both **1** and the initially formed nitrile-coordinated tetrameric species were completely consumed after 60 min of heating at 70 °C, as monitored by the ¹H NMR. The resulting yellow solution showed a single dominant metal hydride peak at δ –12.83 (t, *J* = 18.4 Hz) along with several other minor hydride peaks. The ³¹P NMR also showed a dominant Ru-PCy₃ peak at δ 42.5 ppm.

To determine the molecularity of the “yellow Ru complex”, its diffusion coefficient was compared with several known ruthenium hydride complexes by using diffusion ordered spectroscopy (DOSY) NMR. This method has been successfully utilized in measuring the relative size and molecularity of organometallic complexes.¹⁹ The peak intensity of the Ru–H peaks for **1** (δ –20.7), the dimeric complex [(PCy₃)₂(CO)RuH]₂(μ -OH)(μ -H) (δ –19.4), (PCy₃)₂(CO)RuHCl (δ –24.2), and the yellow complex (δ –12.8) was measured as a function of the gradient field strength (*G*, in Gauss) by using the standard Varian pulse sequence package for DOSY NMR. The plot of $\ln(I/I_0)$ vs *G*² clearly showed that the slope of the hydride peak of the “yellow complex” matched most closely to the monomeric complex (PCy₃)₂(CO)RuHCl (Figure 6), and its diffusion coefficient of 1.3 × 10^{–4} m²/s was quite similar to that of (PCy₃)₂(CO)RuHCl (1.1 × 10^{–4} m²/s). All of these NMR data clearly indicate that the “yellow Ru complex” is a monomeric ruthenium hydride species. Unfortunately, efforts to isolate the “yellow complex” were not fruitful because of its high solubility in nonpolar solvents.

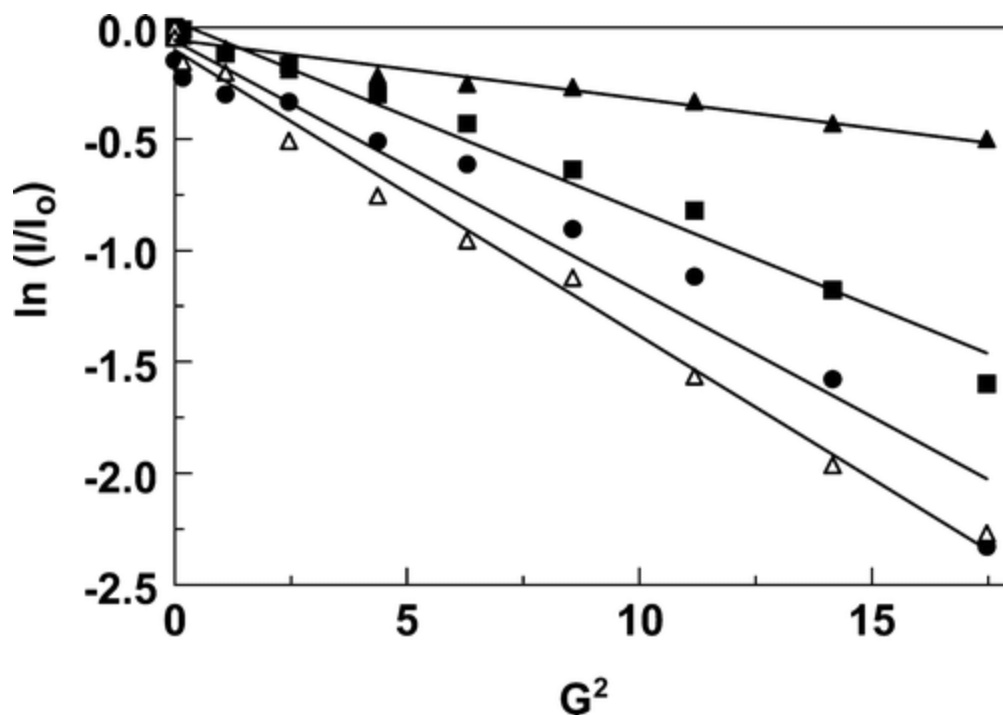


Figure 6. Plots of $\ln(I/I_0)$ vs G^2 obtained from the DOSY NMR. From the bottom, the “yellow Ru complex” **4** (Δ), $(\text{PCy}_3)_2(\text{CO})\text{RuHCl}$ (\bullet), $[(\text{PCy}_3)_2(\text{CO})\text{RuH}]_2(\mu\text{-OH})(\mu\text{-H})$ (\blacksquare), and **1** (\blacktriangle).

A number of alternative mechanisms have also been considered to explain the cooperative activity of the ruthenium catalyst. First, a mechanism involving reversible fragmentation of the tetrameric ruthenium into highly active monomeric and trimeric fragments was considered. However, this mechanism could not readily explain the lack of detectable monomeric species during the hydration of benzonitrile or an unusually high degree of cooperativity ($n > 2$).

In light of the recent reports by Finke and co-workers on colloidal and nanometallic catalysis,²⁰ an autocatalytic mechanism involving colloidal or heterogeneous Ru catalysts was also considered.²¹ A Hg(0) test was performed to resolve the issue of the colloidal/heterogeneous nature of the Ru catalyst. Thus, the hydration reaction of benzonitrile was stirred vigorously in 2-propanol at 80 °C in the presence of **1** (30 mg) and an excess amount of Hg (2.0 g) under otherwise identical reaction conditions as stipulated in eq 1. The amide product was obtained in 95% yield after 6 h of reaction time without any noticeable reduction of the catalytic activity. Certainly, these results are consistent with the homogeneous nature of the ruthenium catalyst, but more careful experiments are needed to rigorously rule out the possibility of an autocatalytic mechanism mediated by a homogeneous ruthenium catalyst.²² To this end, we plan to synthesize a chiral analogue of the catalyst **1** and test its asymmetric induction toward the transfer hydrogenation reaction.

Summary

In summary, we performed detailed kinetic and spectroscopic analyses for the hydration of nitriles catalyzed by the tetrameric ruthenium complex **1**. The sigmoidal kinetics, which was observed for the hydration of electron-poor nitriles, has been successfully described by a three-site modified Hill inhibition equation. The catalytically relevant nitrile-coordinated tetrameric complex **3** was detected by NMR, and the structure of CH_3CN -coordinated complex **3c** was established by X-ray crystallography. In

contrast, noncooperative kinetics was observed for the hydration of electron-rich nitriles, which was satisfactorily described by two-site Michaelis–Menten inhibition kinetics. For this case, a “yellow-colored” ruthenium hydride species was detected, and its monomeric nature was established by DOSY NMR. The electronic nature of the nitrile substrate was found to be the major factor for mediating between cooperative vs noncooperative mechanisms. Our results further suggest that other multinuclear transition metal cluster catalysts with labile ligands could exhibit similar cooperative kinetics.

Experimental Section

General Information

All operations were carried out in an inert-atmosphere glovebox or by using standard high-vacuum and Schlenk techniques unless otherwise noted. Tetrahydrofuran, benzene, hexanes, and Et₂O were distilled from purple solutions of sodium and benzophenone immediately prior to use. The ruthenium complex **1** was prepared by following the reported procedure.¹⁰ The NMR solvents were dried from activated molecular sieves (4 Å). All organic nitriles were received from commercial sources and used without further purification. The NMR spectra were recorded on Varian 300 and 400 MHz FT-NMR spectrometers. Mass spectra were recorded from a Hewlett-Packard HP 5970 GC/MS spectrometer. High-resolution mass spectra were performed at the Center of Mass Spectrometry, Washington University, St. Louis, MO. Elemental analyses were performed at the Midwest Microlab, Indianapolis, IN.

General Procedure of the Catalytic Nitrile Hydration Reaction

A nitrile substrate (2.0 mmol), H₂O (10–20 equiv), and 2–3 mL of solvent were placed in a 25 mL Schlenk tube equipped with a magnetic stirring bar and Teflon stopcock. After the reaction tube was degassed in a dry ice/acetone bath, the reaction tube was brought into the glovebox. The catalyst **1** (34 mg, 1 mol %) was added to the reaction tube. The tube was brought out of the glovebox and was stirred in an oil bath at 80–95 °C for 6–20 h. After the reaction was completed, the reaction tube was opened to air and the solution was filtered through a small pad of Celite. Analytically pure product was isolated by simple recrystallization (*i*-PrOH/hexanes or EtOH/benzene) or by column chromatography on silica gel (EtOAc/hexanes).

Representative Procedure for Measuring the Rate of Hydration Reaction

PhCN (0.05–0.70 mmol) and distilled H₂O (55 μL) were added via syringe to a J-Young NMR tube equipped with a Teflon-coated screw cap containing 2-propanol-*d*₈ (0.3 mL) and benzene-*d*₆ (0.18–0.24 mL). After degassing in a dry ice/acetone bath, the reaction tube was brought into the glovebox, and **1** (4 mg) was added to the tube. The reaction tube was brought out of the glovebox and was immersed in an oil bath that was preset at 80 °C. The tube was removed from the oil bath at 15 min intervals and immediately cooled in a dry ice/acetone bath. The rate of the product formation was determined by ¹H NMR by measuring the integration of the appearance of the product peak at δ 8.3–8.2 (Ph_{meta}) vs the disappearance of the nitrile peak at δ 7.9–7.8 (Ph_{meta}). The initial rate (*v*_i) was obtained from a first-order plots of [PhCN] vs time. The data set was fit to the three-site Hill inhibition kinetics equation by using a nonlinear regression graphing program (ProStat version 4.1).

Hammett Study

A *para*-substituted benzonitrile *p*-X-C₆H₄CN (0.05–0.70 mmol), distilled H₂O (55 μ L), and hexamethylbenzene (2 mg, internal standard) were added to a J-Young NMR tube equipped with a Teflon-coated stopcock in 2-propanol-*d*₈ (0.30 mL) and C₆D₆ (0.18–0.24 mL). The tube was degassed in a dry ice/acetone bath and brought into the glovebox. Complex **1** (4 mg, 2.4 μ mol) was added to the tube. The reaction tube was brought out of the glovebox and was immersed in an oil bath that was preset at 80 °C. The tube was removed from the oil bath at 15 min intervals and immediately cooled in a dry ice/acetone bath. The initial rate of the reaction was determined from pseudo-first-order plots of product formation vs time at each nitrile concentration over a period of 1 h. Each data set was fit to either the Hill or Michaelis–Menten equation by using a nonlinear regression program (ProStat version 4.1).

PCy₃ Inhibition Kinetics Study

A J-Young tube equipped with a Teflon-coated screw cap was charged with benzonitrile (0.05–0.70 mmol), distilled H₂O (55 μ L), and **1** (4 mg) in 2-propanol-*d*₈ (0.3 mL) and C₆D₆ (0.18–0.24 mL) following the above kinetic measurement procedures. A predissolved C₆D₆ solution of PCy₃ (12 μ L, 0.59 M, 1.0 equiv) was syringed into the tube. The tube was sealed and brought out of the glovebox. After an initial ¹H NMR was taken at room temperature, the tube was placed in an oil bath preset at 80 °C. The initial rate was determined from the first-order plot as described above. The same procedure was repeated for 0.25 (1.3 μ L), 0.5 (6 μ L), and 1.5 equiv (21 μ L) of the PCy₃ solution for each nitrile concentration. An analogous procedure was performed for the hydration of methacrylonitrile (0.05–0.70 mmol) by using 0.16, 0.5, 1.0, 1.34, and 1.5 equiv of PCy₃. Each data set was fitted to the inhibition equation by using a nonlinear regression program (ProStat version 4.1).

Diffusion Ordered Spectroscopy (DOSY) NMR Experiment

In separate J-Young tubes, 30 mg of the ruthenium complexes, **1**, [(PCy₃)₂(CO)RuH]₂(μ -OH)(μ -H), (PCy₃)₂(CO)RuHCl, and the “yellow Ru complex” were dissolved in toluene-*d*₈. The tubes were sealed and placed in a NMR probe at 20 °C. The standard Varian DOSY pulse sequence Dbppste (bipolar pulse pair simulated echo experiment) was used to measure the ruthenium hydride peak heights at each gradient level. The pulse delay between the gradients was kept constant at 5 ms as the *z* gradient was varied from 10 to 1000 (gzl). The initial intensity (*I*₀) for the Ru–H peaks was determined at each *z* gradient, and the peak height intensity was normalized by using the peak height function of the VNMRJ program. The linear regression fit for the plots of ln(*I*/*I*₀) vs *G*² (in Gauss) was used to determine the diffusion coefficients for each complex.

Acknowledgment

Financial support from the NIH’s National Institute of General Medical Sciences (Grant R15 GM55987) is gratefully acknowledged. We thank Prof. Daniel Sem for helpful suggestions on the kinetic analysis.

Supporting Information

Kinetic analysis and crystallographic data of **3c**. This material is available free of charge via the Internet at <http://pubs.acs.org>.

References

- ¹ Recent reviews: (a) Robertson, A.; Shinkai, S. *Coord. Chem. Rev.* 2000, 205, 157.
(b) Kovbasyuk, L.; Krämer, R. *Chem. Rev.* 2004, 104, 3161.
- ² (a) *Catalysis by Di- and Polynuclear Metal Cluster Complexes*; Adams, R. D.; Cotton, F. A., Eds.; Wiley-VCH: New York, 1998.
(b) *Multimetallic Catalysts in Organic Synthesis*; Shibasaki, M.; Yamamoto, Y., Eds.; Wiley-VCH: Weinheim, 2004.
- ³ (a) Hidai, M.; Kuwata, S.; Mizobe, Y. *Acc. Chem. Res.* 2000, 33, 46.
(b) Ready, J. M.; Jacobsen, E. N. *J. Am. Chem. Soc.* 2001, 123, 2687.
(c) Sammis, G. M.; Danjo, H.; Jacobsen, E. N. *J. Am. Chem. Soc.* 2004, 126, 9928.
(d) Ko, S.; Kang, B.; Chang, S. *Angew. Chem., Int. Ed.* 2005, 44, 455.
- ⁴ (a) Jacobsen, E. N. *Acc. Chem. Res.* 2000, 33, 421.
(b) Gianneschi, N. C.; Masar, M. S., III; Mirkin, C. A. *Acc. Chem. Res.* 2005, 38, 825.
- ⁵ (a) Takeuchi, M.; Ikeda, M.; Sugasaki, A.; Shinkai, S. *Acc. Chem. Res.* 2001, 34, 865.
(b) Yamagiwa, N.; Matsunaga, S.; Shibasaki, M. *J. Am. Chem. Soc.* 2003, 125, 16178.
(c) Handa, S.; Gnanadesikan, V.; Matsunaga, S.; Shibasaki, M. *J. Am. Chem. Soc.* 2007, 129, 4900.
- ⁶ (a) Suzuki, H.; Takaya, Y.; Takemori, T.; Tanaka, M. *J. Am. Chem. Soc.* 1994, 116, 10779.
(b) Suzuki, H. *Eur. J. Inorg. Chem.* 2002, 1009.
- ⁷ Adams, R. D.; Captain, B.; Zhu, L. *J. Am. Chem. Soc.* 2006, 128, 13672.
- ⁸ (a) Perutz, M. *Mechanisms of Cooperativity and Allosteric Regulation*; Cambridge University Press: New York, 1989.
(b) Voet, D.; Voet, J. D. *Biochemistry*, 3rd ed.; Wiley: Hoboken, 2004; Chapter 10.
- ⁹ (a) Takeuchi, M.; Imada, T.; Shinkai, S. *Angew. Chem., Int. Ed.* 1998, 37, 2096.
(b) Dubé, C. E.; Wright, D. W.; Armstrong, W. H. *Angew. Chem., Int. Ed.* 2000, 39, 2169.
- ¹⁰ Yi, C. S.; Zeczycki, T. N.; Guzei, I. A. *Organometallics* 2006, 25, 1047.
- ¹¹ See the [Supporting Information](#) for selected spectroscopic data of these products.
- ¹² Selected recent examples: (a) Murahashi, S.-I.; Takaya, H. *Acc. Chem. Res.* 2000, 33, 225.
(b) Breno, K. L.; Pluth, M. D.; Tyler, D. R. *Organometallics* 2003, 22, 1203.
(c) Oshiki, T.; Yamashita, H.; Sawada, K.; Utsunomiya, M.; Takahashi, K.; Takai, K. *Organometallics* 2005, 24, 6287.
- ¹³ Segel, I. H. *Enzyme Kinetics*; Wiley: New York, 1975.
- ¹⁴ (a) King, E. L.; Altman, C. J. *Phy. Chem.* 1956, 60, 1375.
(b) Cha, S. J. *Biol. Chem.* 1968, 243, 820.

- ¹⁵ See the [Supporting Information](#) for the derivation of the Hill and Michaelis–Menten inhibition kinetic equations.
- ¹⁶ Recent examples of two-site Michaelis–Menten kinetics: (a) Corey, E. J.; Noe, M. C. *J. Am. Chem. Soc.* 1996, 118, 319.
(b) Pirrung, M. C.; Liu, H.; Morehead, A. T., Jr. *J. Am. Chem. Soc.* 2002, 124, 1014.
- ¹⁷ The NMR assignment of the metal hydride peaks of **3c** was made by comparing the spectroscopic patterns of **3c** with those of **3a** and **3b** (see the [Supporting Information](#), Table S1).
- ¹⁸ (a) Perutz, M. F. *Mechanism of Cooperativity and Allosteric Regulation in Proteins*; Cambridge University Press: London, 1990.
(b) Cowan, J. A. *Inorganic Biochemistry*; Wiley-VCH: New York, 1997.
- ¹⁹ (a) Viviente, E. M.; Pregosin, P. S.; Schott, D. In *Mechanisms in Homogeneous Catalysis. A Spectroscopic Approach*; Heaton, B., Ed.; Wiley-VCH: Weinheim, 2005.
(b) Williams, C. K.; Breyfogle, L. E.; Choi, S. K.; Nam, W.; Young, V. G., Jr.; Hillmyer, M. A.; Tolman, W. B. *J. Am. Chem. Soc.* 2003, 125, 11350.
(c) Pregosin, P. S.; Martney-Viviente, E. M.; Kumar, P. G. A. *Dalton Trans.* 2003, 4007.
(d) Casey, C. P.; Johnson, J. B.; Singer, S. W.; Cui, Q. *J. Am. Chem. Soc.* 2005, 127, 3100.
- ²⁰ (a) Widegren, J. A.; Bennett, M. A.; Finke, R. G. *J. Am. Chem. Soc.* 2003, 125, 10301.
(b) Hagen, C. M.; Widegren, J. A.; Maitlis, P. M.; Finke, R. G. *J. Am. Chem. Soc.* 2005, 127, 4423.
(c) Hagen, C. M.; Vieille-Petit, L.; Laurency, G.; Süß-Fink, G.; Finke, R. G. *Organometallics* 2005, 24, 1819.
- ²¹ For recent reviews of colloidal and nanometallic catalysts: (a) Schulz, J.; Roucoux, A.; Patin, H. *Chem. Rev.* 2002, 102, 3757. (b) Moreno-Manas, M.; Pleixats, R. *Acc. Chem. Res.* 2003, 36, 638.
- ²² A number of autocatalytic mechanisms mediated by homogeneous metal catalysts have been proposed recently. For recent selected examples:
(a) Hadzovic, A.; Song, D.; MacLaughlin, C. M.; Morris, R. H. *Organometallics* 2007, 26, 5987.
(b) Smith, S. E.; Sasaki, J. M.; Bergman, R. G.; Mondloch, J. E.; Finke, R. G. *J. Am. Chem. Soc.* 2008, 130, 1839.
- For recent reviews on asymmetric autocatalytic chiral amplification mechanisms:
(c) Soai, K.; Shibata, T.; Sato, I. *Acc. Chem. Res.* 2000, 33, 382.
(d) Kondepudi, D. K.; Asakura, K. *Acc. Chem. Res.* 2001, 34, 946.
(e) Blackmond, D. G. *Prog. Nat. Acad. Sci.* 2004, 101, 5732.